Decision Making and Analysis
https://ojs.luminescience.cn/DMA

LUMINESCIENCE
https://luminescience.cn

Research Article

Bias regulation in algorithmic decision systems: a metaheuristic intervention for business development decisions

Yu-Min Wei

Independent Researcher, 545301, Puli, Taiwan

Corresponding to: Yu-Min Wei, Email: weiyumin.research@gmail.com

Abstract: Metaheuristic decision systems can develop exploration-exploitation imbalance under cognitive bias. Existing decision research examines outcomes, adaptive search control, and bias reduction but gives limited attention to internal search structure. This study develops the Metaheuristic-Based Bias Intervention Module as a decision analysis artifact that combines genetic algorithm and particle swarm optimization search with cognitive bias mechanisms, bounded parameter control, and structural indicators. Controlled experiments compare a genetic algorithm, a fixed hybrid configuration, and the proposed module across simulated business development allocation scenarios. Results show that the proposed module preserves decision accuracy and bias reduction while improving symmetry and convergence stability relative to the fixed hybrid configuration. Recorded parameter changes confirm controller activity, while calibration tests and comparisons with entropy, proportional balance, and population diversity support symmetry as a measure of search structure. Exchange symmetry contributes a measurable property of search allocation under cognitive bias and distinguishes structural balance from outcome quality. Integrating adaptivity, symmetry, stability, bias reduction, and accuracy creates a process-level diagnostic structure for decision analysis. Practical relevance lies in a proposed diagnostic logic for search concentration and potential intervention points in partner selection, investment prioritization, and opportunity evaluation. The computational framework provides a foundation for subsequent organizational research on contextual calibration, managerial utility, and decision quality.

Keywors: Symmetry regulation, Exploration-exploitation, Cognitive bias, Metaheuristic decision systems, Decision analysis, Business development

1. Introduction

Decision-making under uncertainty can rely on heuristic or eristic shortcuts [1]. Cognitive biases affect professional decision-making across multiple occupational domains [2]. Evolutionary algorithms combine exploration and exploitation as core search functions [3]. Information retrieval research identifies familiarity and anchoring among biases that can shape search behavior [4]. Behavioral decision research documents overconfidence, anchoring, and other cognitive biases across professional settings [2]. The present study treats such directional distortions as potential sources of asymmetric decision trajectories. Bounded rationality remains relevant to managerial decision making despite greater data availability [5]. Fast-and-frugal heuristics provide simple decision rules for choices under uncertainty [6].

Research on managerial heuristics and biases examines

Received: Jul. 15, 2026; Revised: Aug. 24, 2026; Accepted: Sept. 22, 2026; Published: Sept. 24, 2026
Copyright © 2026 Yu-Min Wei.
DOI: https://doi.org/10.55976/dma.420261638110-132
This is an open-access article distributed under a CC BY license (Creative Commons Attribution 4.0 International License)
https://creativecommons.org/licenses/by/4.0/
A previous version of this manuscript was deposited as a preprint on Preprints.org, DOI: https://doi.org/10.20944/preprints202601.0816.v1.

how cognitive shortcuts shape judgment and decision making [7]. Emerging technologies such as artificial intelligence, data analytics, and digital platforms shape organizational processes and interdependencies [8]. Algorithmic management systems can perform functions such as monitoring, goal setting, performance management, and scheduling [9]. The law of requisite variety links regulatory capacity to the variety confronting a complex system [10]. This principle provides a basis for examining adaptive regulation in algorithmic decision processes.

Recent research on collective decision-making shows that symmetry breaking can emerge when interactions differentiate otherwise equivalent options [11]. In metaheuristic optimization, exploration and exploitation constitute complementary search functions whose balance is central to algorithm design and performance [3, 12]. The present study treats symmetry as a structural property of their proportional relation rather than as a measure of decision optimality. Equal normalized levels represent exact proportional symmetry, whereas dominance by either search function represents asymmetry. This formulation allows the analysis to examine changes in search structure under cognitive bias without assuming that greater symmetry produces better decisions.

Metaheuristic algorithms provide a computational structure for search intervention [13]. These algorithms coordinate exploration and exploitation through iterative search and evaluation [12, 14]. Exploration identifies potential directions, while exploitation refines promising regions [15]. Behavioral research distinguishes directed and random exploration as strategies for addressing the exploration-exploitation dilemma [16]. Organizational learning research shows that self-confirming biased beliefs can lock learning processes into suboptimal actions, while exploration can help agents escape these beliefs [17]. Experimental evidence shows that premature exploitation can perpetuate initial cognitive biases [18]. The present study represents such search imbalance through exchange symmetry. Symmetry formalizes invariance under a specified operation, including the permutation of system components [19]. In the present representation, the exchange operation interchanges the normalized exploration and exploitation components. The resulting symmetry measure remains invariant under this exchange, while exact state symmetry occurs when the two components have equal values. Departures from equality indicate asymmetry, and the sign of their difference identifies which search function dominates.

Optimization research has combined genetic and swarm mechanisms within computational search architectures [20], and comparative studies have examined the search characteristics of Genetic Algorithm (GA) and Particle Swarm Optimization (PSO) [21]. Building on these foundations, this study introduces the Metaheuristic-Based Bias Intervention Module (MBIM) to examine bias-affected exploration-exploitation structure in algorithmic decision processes. Modified PSO research shows that evolutionary operators and control hyperparameters can reshape convergence behavior and support adaptation across problem settings [22]. MBIM applies adaptive parameter control to regulate search dynamics and treats symmetry as a property of the search process. Metaheuristic research has examined asymmetric objective structures, including trade-offs between cost and reliability [23]. The present study uses exchange symmetry to assess proportional changes in exploration and exploitation and relates these changes to convergence stability (CS) under cognitive bias.

Methodological grounding follows a Design Science Research (DSR) approach [24, 25]. This study develops a computational artifact that regulates bias-affected search structure at the process level. Metaheuristic research distinguishes population-based approaches from single-solution methods and provides established computational structures for complex search problems [26]. MBIM builds on population-based search mechanisms to examine exploration-exploitation structure under cognitive bias. The study defines the Symmetry Regulation Index (SRI) to assess proportional equality in exploration-exploitation allocation across iterations. Research on complex adaptive systems emphasizes interacting components that adapt or learn through their interactions [27]. In the present evaluation, CS and bias reduction complement SRI by characterizing distinct properties of the resulting decision trajectories. These measures enable joint assessment of outcome attainment, search structure, and computational operation across metaheuristic configurations.

This research addresses an integrative gap in the process-level analysis of algorithmic decision systems affected by cognitive bias. Prior metaheuristic research has examined exploration-exploitation balancing through explicit search control, diversity measurement, parameter configuration, and hybrid architecture design [3, 12, 28, 29]. Behavioral decision research documents the effects of cognitive bias on professional judgment [2]. Experimental research links exploitation-oriented search to the maintenance of cognitive biases [18]. Limited integration of these research streams leaves unclear how bias-induced distortion of search allocation relates to proportional structure, CS, bias reduction, and decision accuracy (DA) within algorithmic decision processes.

These gaps motivate the following research question.

How can an algorithmic decision system regulate symmetry after cognitive bias disrupts the balance between exploration and exploitation, and how can metaheuristic mechanisms operationalize such regulation at the process level?

To address this question, the study develops and evaluates a computational structure that integrates adaptive metaheuristic mechanisms with symmetry-based evaluation. The resulting decision-support module examines bias-responsive parameter adjustment and its effects on search structure under controlled simulation.

This work makes theoretical, methodological, and

applied contributions. Theoretically, it positions symmetry as a measurable property of algorithmic decision processes. Methodologically, it develops a decision-analysis artifact that integrates established Genetic Algorithm-Particle Swarm Optimization (GA-PSO) search mechanisms, bias characterization, and an adaptive parameter controller. Population diversity, search stagnation, and anchor concentration guide bounded parameter adjustments, while process-level indicators evaluate the resulting decision dynamics under cognitive bias. Applied research can use the framework to examine business development decision processes shaped by uncertainty and feedback complexity [30, 31].

2. Literature review

2.1 Foundations of symmetry in decision systems

Managerial decision research identifies data quality, utility, and value as continuing limitations on decision making [5]. Behavioral decision research shows that cognitive biases affect professional judgment and decision-making [2]. Metaheuristic research examines explicit control of exploration and exploitation during search [3].

Decision-making involves a recurring trade-off between exploiting known options and exploring alternatives [32]. Behavioral research documents optimism bias, overconfidence, anchoring, and escalation of commitment in project decision making [33].

Symmetry regulation extends the analytical treatment of exploration and exploitation without proposing an alternative exploration-exploitation theory. Existing research examines how search processes allocate and adjust exploration and exploitation [3, 12, 28]. Population diversity provides one approach for characterizing this balance in population-based metaheuristics [29]. A symmetry perspective addresses the structural form produced by this allocation. Computational research defines symmetry as invariance under a specified transformation [19]. The present study applies exchange invariance to normalized exploration and exploitation. Proportional equality constitutes exact symmetry, and departure from equality measures structural asymmetry. Component differences identify the direction of dominance. Cognitive bias can sustain exploitation of a favored option and restrict the search for alternatives, which supports this directional interpretation [18]. This structural representation distinguishes symmetry from search performance and decision optimality.

Recent advances in computational decision systems introduce metaheuristics as mechanisms capable of monitoring deviation and restoring balance in dynamic environments [34, 35]. The integration of cognitive theory, optimization logic, and symmetry constructs establishes the foundation for this study.

2.2 Symmetry breaking through cognitive bias

Research across evolutionary algorithms and human decision making examines how decision processes allocate between exploration and exploitation [3, 32]. The present study interprets bias-induced shifts in this relation as symmetry breaking. Bias originates from heuristic processing that simplifies reasoning under cognitive limitation [2, 5].

Behavioral strategy research links mental processes and behavioral bounds to strategic agency and the pursuit of opportunities [36]. Overconfidence reflects excessive confidence in one's own judgments [33]. Self-enhancing responses to diverging performance indicators can preserve perceptions of success and reduce willingness to change [37]. Anchoring restricts conceptual search. Confirmation bias reinforces initial assumptions and reduces adaptive correction [38].

Management decisions under radical uncertainty can arise when managers lack probabilistic and qualitative information and cannot rely on familiar heuristic cues [39]. Experimental evidence on intertemporal choice shows that group collaboration can reduce delay discounting and promote farsighted choices [40]. An integrative review of organizational bias mitigation distinguishes debiasing from choice architecture and identifies limited comparative evidence across these approaches [41].

2.3 Metaheuristics as symmetry regulation mechanisms

Studies of collective decision-making show that higher-order interactions can break symmetry among equivalent options [11], while research on statistical systems examines symmetry breaking and local symmetry restoration [42]. The present study applies these symmetry concepts to the proportional relation between exploration and exploitation in metaheuristic search. These algorithms rely on iterative sampling, feedback, and search coordination to navigate large and complex solution spaces [28, 43]. Exploration expands the range of potential directions, whereas exploitation concentrates search effort on promising regions [3, 12]. Population diversity provides an established indicator for characterizing the exploration-exploitation balance in population-based metaheuristics [29].

A wide range of metaheuristic designs implement distinct strategies for regulating search behavior. GA, PSO, Ant Colony Optimization, Firefly Algorithm, and Gravitational Search Algorithm differ in how they allocate search effort, coordinate candidate solutions, and stabilize convergence patterns over time [44-46]. These design choices influence the coherence of diversification and intensification within decision processes, rather than directing search toward a single optimal configuration or a balanced terminal state.

Research on learning-enhanced metaheuristics examines adaptive parameter and operator control [28]. GA surveys document the role of operator and parameter configuration

in applied search problems [47]. An integrative review examines interventions that mitigate cognitive bias in organizational decisions [41]. Work on symmetry breaking and restoration analyzes how statistical systems lose and recover local symmetry [42]. The MBIM adopts GA-PSO hybridization as an established search architecture and directs its contribution toward the process-level analysis of bias-affected algorithmic decision systems. Its distinctive role concerns the representation of cognitive bias as directional distortion in search allocation and the comparison of proportional structure, CS, bias reduction, and DA across fixed metaheuristic configurations.

2.4 Design science as an implementation methodology

DSR provides a methodological structure for developing and evaluating computational intervention systems that address organizational decision problems [24]. This approach centers on artifacts that integrate behavioral insight with technical design and evaluates performance through task-relevant criteria grounded in use contexts [48]. Within this methodology, researchers specify design objectives, construct artifacts, and assess outcomes through systematic comparison of configurations under controlled conditions [49].

A metaheuristic module functions as such an artifact by structuring search behavior and regulating decision dynamics in the presence of bias and uncertainty [13, 43]. DSR supports iterative refinement of artifact architecture and disciplined evaluation of process-level behavior through context-appropriate evidence. Responsible data science identifies fairness, accuracy, confidentiality, and transparency as central concerns in data-driven systems [50]. Machine-learning research identifies biases in data and algorithms as sources of unfair outcomes and examines approaches to fairness and bias mitigation [51]. This methodological perspective enables integration of behavioral theory, metaheuristic design, and symmetry constructs within a coherent intervention architecture [52, 53].

2.5 Integrated perspective

Research on symmetry breaking and restoration provides a basis for examining structural change in system states [42]. Metaheuristic research addresses the organization of computational search across complex solution spaces [43], while machine-learning research examines bias and fairness in algorithmic systems [51]. The present study brings these streams together to examine regulated decision behavior. Cognitive bias enters the model as directional distortion in search allocation, and metaheuristics organize exploration and exploitation within the decision process. DSR provides the methodological framework for implementing and evaluating the resulting computational artifact [48, 49].

These streams operate at distinct analytical levels. Behavioral decision research frames choice as a trade-off between exploiting known options and exploring alternatives [32], whereas metaheuristic research examines search allocation, diversity, and convergence [3, 29]. Metaheuristic literature treats the exploration-exploitation balance as a core design concern and notes the limited availability of accepted and reproducible metrics [12]. Permutation-equivariant research provides a formal example of computational models that encode symmetry under component permutations [19]. The present study applies an exchange operation to normalized exploration and exploitation and defines invariance under that exchange. Design science connects artifact behavior with explicit evaluation criteria [48]. Decision-oriented explainable artificial intelligence research treats predictive reliability, explanatory fidelity, and stakeholder usefulness as distinct concerns in algorithmic decision support [54]. No Free Lunch results show that algorithm performance depends on the problem class [55]. The present framework relates bias, parameter control, symmetry, convergence, and outcome measures under configuration-specific search conditions.

2.6 Research gap and link to methodology

Recent decision research examines how stakeholder bias affects group decision dynamics [56], while metaheuristic research provides established accounts of exploration-exploitation dynamics [57]. Metaheuristic research examines adaptive search control, diversity preservation, parameter configuration, and hybrid architecture. Behavioral and computational perspectives create an integrative research opportunity concerning the process-level representation of bias-induced search allocation in algorithmic decision systems.

This study addresses this integrative research opportunity through the MBIM. Established GA-PSO mechanisms provide the computational structure, while symmetry regulation, CS, bias reduction, and DA support comparative analysis across the three nested search configurations. Integration of these elements connects cognitive bias with observable search dynamics and positions the contribution at the level of decision-process analysis.

Symmetry regulation denotes the monitoring and adjustment of the exploration-exploitation relation during iterative search. SRI records proportional equality, while the exploration and exploitation values identify the direction of dominance. A symmetry profile gains decision significance through joint interpretation with DA, bias reduction, CS, algorithmic efficiency (AE), and adaptivity.

3. Materials and methods

3.1 Research design

This study applies a DSR methodology to construct and evaluate the MBIM. DSR provides a structured

approach for developing computational artifacts grounded in theoretical reasoning and systematic evaluation [24, 48]. The research assumes that cognitive bias introduces asymmetry into decision behavior and that the study examines and regulates such asymmetry through structural configuration of metaheuristic search processes, rather than through prescriptive correction of decision outcomes.

The research design proceeds through three sequential phases. MBIM construction initiates the process through a hybrid GA and PSO architecture that defines exploration-exploitation dynamics at the process level. Controlled simulation experiments provide a basis for comparison across the three nested search configurations under bias conditions. Such a design constitutes an ex post artificial evaluation of the instantiated artifact [58]. Stability-oriented and comparative criteria guide assessment of decision trajectories, convergence patterns, and symmetry-related indicators. Table 1 summarizes the phases and their corresponding objectives.

Table 1. Overview of research design

DSR stage	Objective	Key activity	Output/Artifact	Evaluation method
Problem identification	Identify structural imbalance in decision processes under cognitive bias	Literature review and analytical synthesis	Bias characterization	Conceptual consistency check
Objective definition	Define analytical objectives for symmetry regulation	Mapping relations between bias and exploration-exploitation structure	Symmetry representation	Internal coherence review
Design and development	Develop the MBIM	GA-PSO search with adaptive parameter control	Executable adaptive MBIM	Functional verification
Demonstration	Examine module behavior through computational experiments	Controlled decision scenarios	Experimental outcomes	Comparative configuration analysis
Evaluation	Assess technical and analytical utility	Paired computational experiments, sensitivity analysis, and indicator validation	Comparative evidence on artifact behavior	Ex post artificial evaluation
Communication	Report findings and theoretical implications	Academic writing and dissemination	Research manuscript	Scholarly review process

3.2 Conceptual foundation for symmetry regulation

The conceptual foundation rests on three theoretical elements that together define the analytical scope of the artifact. Evidence from behavioral research documents the effects of cognitive bias on judgment and decision making under uncertainty [2, 59, 60]. Metaheuristic design provides structured search processes that organize exploration and exploitation within complex decision spaces [57, 61]. Diversity metrics in population-based metaheuristics characterize the exploration-exploitation balance [29]. This study represents proportional balance through symmetry and examines its relation to CS.

The artifact operationalizes symmetry regulation through bounded control of the search parameters. Cognitive disturbance shapes the initial trajectory. Diversity loss, stagnation, and anchor concentration supply controller signals, while parameter updates alter search allocation. SRI evaluates the resulting proportional relation as a structural outcome. DA, bias reduction, CS, efficiency, and adaptivity determine its performance significance.

The conceptual foundation links behavioral distortion, computational structure, and evaluative indicators within a single analytical system. Cognitive bias defines the form of asymmetry, metaheuristic configuration regulates process dynamics, and symmetry measures describe structural outcomes of search behavior. This alignment enables systematic examination of regulated decision processes while separating adaptive parameter control from direct outcome correction.

3.3 Artifact specification

Metaheuristic research encompasses hundreds of nature-inspired algorithms and recognizes modification and hybridization as established design directions [62, 63]. The present study combines GA and PSO within MBIM

to structure search behavior. Population-based variation in GA supports broad exploration, whereas coordinated particle movement in PSO shapes convergence across candidate solutions. Multicriteria decision research applies formal decision methods to innovation assessment in small and medium-sized enterprises and covers business strategy, management, and technology selection [64]. The experiment uses partner screening, investment prioritization, and opportunity evaluation as simulated business development settings for controlled comparison across configurations.

Four coordinated components organize the artifact's internal operation. Research on organizational decisions examines interventions for mitigating cognitive bias [41], while decision research considers strategies for improving bounded judgment [65]. Strategic cognition research incorporates cognitive and emotional processes into explanations of organizational adaptation [66]. The present model represents anchoring, confirmation bias, and overconfidence through the transition rules in Equations (8)-(10). Search coordination executes GA and PSO routines under fixed or controller-adjusted parameter settings. Research on learning-enhanced metaheuristics identifies adaptive parameter and operator control as established mechanisms for adjusting search behavior [28], while diversity metrics characterize candidate dispersion in population-based metaheuristics [29]. The adaptive configuration interface uses population diversity, search stagnation, and anchor concentration as inputs for bounded parameter adjustments during MBIM execution. Symmetry assessment uses SRI to measure proportional equality across exploration and exploitation trajectories.

Established GA-PSO search mechanisms provide the computational foundation for the artifact. MBIM organizes bias characterization, search coordination, adaptive configuration control, and symmetry assessment as an integrated decision-analysis architecture. Population diversity, search stagnation, and anchor concentration guide bounded parameter adjustments during execution. Its artifact contribution resides in connecting adaptive search control with process-level analysis of algorithmic decision dynamics.

Figure 1 presents the artifact architecture and the feedback relation among bias characterization, GA-PSO search, adaptive parameter control, and process-level assessment.

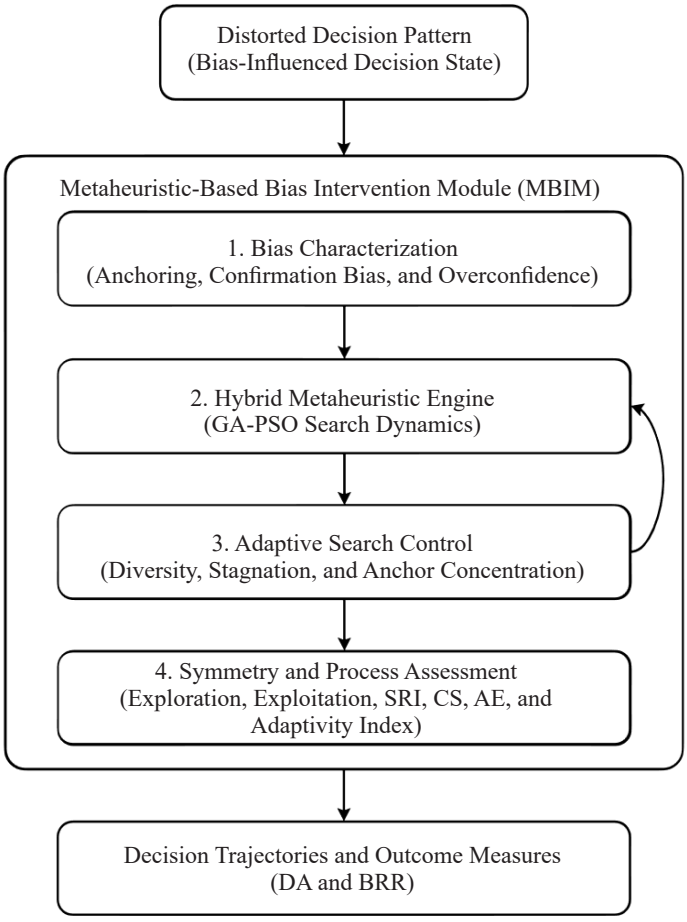


Figure 1. Architecture and feedback operation of the MBIM

3.4 Mathematical representation

3.4.1 Decision space and objective function

Each candidate solution represents an allocation across n decision alternatives. The allocation vector belongs to the probability simplex:

$$\mathrm{x} \in \Delta^{n-1} = \left\{ \mathrm{x} \in \mathbb{R}^n \middle| x_i \geq 0,\ \sum_{i=1}^{n} x_i = 1 \right\} \tag{1}$$

Matrix $\mathrm{A} \in [0,\ 1]^{n \times m}$ contains the attributes of n alternatives across m decision criteria. Vector $\mathrm{w} \in \Delta^{m-1}$ contains the criterion weights. The weighted utility vector is:

$$\mathrm{u} = \mathrm{Aw} \tag{2}$$

Decision quality combines weighted utility and allocation risk:

$$F(\mathrm{x}) = \mathrm{u}^{\top}\mathrm{x} - \rho \mathrm{x}^{\top}\mathrm{Rx} \tag{3}$$

Matrix $\mathrm{R} \in \mathbb{R}^{n \times n}$ is positive semidefinite and represents risk dependence across the decision alternatives. Parameter $\rho > 0$ controls risk aversion. Each configuration maximizes $F(\mathrm{x})$ under the feasibility conditions in Equation (1). The quadratic risk term penalizes allocations with greater risk exposure, while simplex projection preserves nonnegative allocation shares with a unit sum.

3.4.2 GA and PSO updating mechanisms

GA chromosomes use the real-valued allocation vectors defined in Equation (1), and the same vectors serve as PSO particle positions. Equation (3) supplies the fitness values used for selection, replacement, and best-record updates. The GA uses tournament selection with three candidates, two-solution elitism, blend crossover, and Gaussian mutation. For parent vectors $\mathrm{x}_{i,\,t}^{(1)}$ and $\mathrm{x}_{i,\,t}^{(2)}$, blend crossover produces:

$$\mathrm{y}_{i,\,t} = \alpha_{i,\,t} \odot \mathrm{x}_{i,\,t}^{(1)} + \left(1 - \alpha_{i,\,t}\right) \odot \mathrm{x}_{i,\,t}^{(2)} \tag{4}$$

The vector $\alpha_{i,\,t} \in [0,\ 1]^n$ contains crossover weights. Mutation changes the offspring according to:

$$\mathrm{x}_{i,\,t+1} = \Pi_{\Delta}\left(\mathrm{y}_{i,\,t} + \mathrm{m}_{i,\,t} \odot \eta_{i,\,t}\right) \tag{5}$$

Vector $\mathrm{m}_{i,\,t} \in \{0,\ 1\}^n$ contains Bernoulli mutation indicators, $\eta_{i,\,t} \sim \mathcal{N}\left(0,\ \sigma_{m,\,t}^2 \mathrm{I}\right)$, and Π_{Δ} denotes projection onto the probability simplex. The GA configuration uses a crossover probability of 0.90, a mutation probability of $1/n$, and a mutation scale of 0.06.

The PSO component updates particle velocity through:

$$\mathrm{V}_{i,\,t+1} = \omega_t \mathrm{V}_{i,\,t} + c_{1,\,t}\mathrm{r}_{1,\,i,\,t} \odot (\mathrm{p}_{i,\,t} - \mathrm{x}_{i,\,t}) + c_{2,\,t}\mathrm{r}_{2,\,i,\,t} \odot (\mathrm{g}_t - \mathrm{x}_{i,\,t}) \tag{6}$$

Vector $\mathrm{p}_{i,\,t}$ denotes the best solution recorded by particle i, g_t denotes the best solution recorded by the population, and the elements of $\mathrm{r}_{1,\,i,\,t}$ and $\mathrm{r}_{2,\,i,\,t}$ follow a uniform distribution on [0, 1]. The velocity limit is 0.20. Particle position follows:

$$\mathrm{X}_{i,\,t+1} = \Pi_{\Delta}\left(\mathrm{X}_{i,\,t} + \mathrm{V}_{i,\,t+1}\right) \tag{7}$$

The fixed GA-PSO configuration uses $\omega = 0.70$ and $c_1 = c_2 = 1.50$. PSO updates the complete population during each iteration. GA operators replace the lowest-performing half of the population after every five PSO iterations. The replacement procedure uses the same crossover and mutation settings as the GA configuration.

Each hybrid iteration evaluates the current population, retrieves the personal and population best records, and applies one PSO transition to all particles. Fitness reevaluation follows the cognitive-bias transformation of the proposed positions. Every fifth iteration, tournament selection draws 25 parents from the updated population. Blend crossover and Gaussian mutation generate 25 offspring, which replace the 25 candidates with the lowest fitness. Replacement resets the corresponding velocities to zero and applies the same bias transformation to the offspring. Final fitness evaluation updates the personal and population best records. Fixed GA-PSO retains constant parameters, while MBIM supplies iteration-specific values from Equations (15)-(17).

3.4.3 Cognitive-bias disturbances

Each search configuration receives the same cognitive-bias disturbance after a proposed GA or PSO transition. Vector $\mathrm{a} \in \Delta^{n-1}$ represents the initial anchor, $b \in [0,\ 1]$ represents bias strength, and $\mathrm{x}_{i,\,t+1}^{p}$ represents the proposed candidate position. Anchoring produces:

$$\tilde{\mathrm{x}}_{i,\,t+1} = \Pi_{\Delta}\left[\mathrm{x}_{i,\,t+1}^{p} + 0.035b\left(\mathrm{a} - \mathrm{x}_{i,\,t+1}^{p}\right)\right] \tag{8}$$

Confirmation bias attenuates a proposed transition that increases distance from the anchor. Let $B_{i,\,t}$ ~ Bernoulli($0.55b$). The disturbed position is:

$$\tilde{\mathrm{x}}_{i,\,t+1}=\begin{cases}\Pi_{\Delta}\left(0.75\mathrm{x}_{i,\,t}+0.25\mathrm{x}_{i,\,t+1}^{p}\right), & \left\|\mathrm{x}_{i,\,t+1}^{p}-\mathrm{a}\right\|_{2}>\left\|\mathrm{x}_{i,\,t}-\mathrm{a}\right\|_{2} \text{ and } B_{i,\,t}=1,\\ \mathrm{x}_{i,\,t+1}^{p}, & \text{otherwise.}\end{cases} \tag{9}$$

Overconfidence increases allocation concentration through a power transformation:

$$Z_{ij,\,t+1}=\left(\max\{x_{ij,\,t+1}^{p},\ \varepsilon\}\right)^{1+0.20b},\ \tilde{\mathrm{x}}_{i,\,t+1}=\Pi_{\Delta}(\mathrm{Z}_{i,\,t+1}) \tag{10}$$

The three disturbances alter candidate transitions without changing the objective function in Equation (3). This common treatment isolates the effect of search coordination and parameter control across the experimental configurations.

3.4.4 MBIM adaptive controller

MBIM converts population diversity, search stagnation, and anchor concentration into an exploration-demand signal. Population diversity at iteration t is:

$$D_t=\frac{1}{N\sqrt{2}}\sum_{i=1}^{N}\left\|\mathrm{x}_{i,\,t}-\bar{\mathrm{x}}_{t}\right\|_{2},\ \bar{\mathrm{x}}_{t}=\frac{1}{N}\sum_{i=1}^{N}\mathrm{x}_{i,\,t} \tag{11}$$

Anchor concentration is:

$$q_t=\frac{1}{N}\sum_{i=1}^{N}\left(1-\frac{\left\|\mathrm{x}_{i,\,t}-\mathrm{a}\right\|_{2}}{\sqrt{2}}\right) \tag{12}$$

Normalized diversity and stagnation signals follow:

$$d_t=\min\left\{1,\ \frac{D_t}{D_0}\right\},\ s_t=\min\left\{1,\ \frac{L_t}{20}\right\},\ 0\le d_t,\ s_t\le 1 \tag{13}$$

Variable L_t counts consecutive iterations without an objective improvement greater than 10^{-5}. Exploration demand combines the three signals:

$$r_t=\min\left\{1,\ 0.45(1-d_t)+0.30s_t+0.25q_t\right\} \tag{14}$$

The controller sets the PSO parameters as:

$$\omega_t=0.40+0.50r_t,\ c_{1,\,t}=1.10+0.90r_t,$$

$$c_{2,\,t}=2.00-0.90r_t \tag{15}$$

The crossover and mutation probabilities are:

$$p_{c,\,t}=0.65+0.30r_t,\ p_{m,\,t}=0.02+0.23r_t \tag{16}$$

Mutation scale is:

$$\sigma_{m,\,t}=0.02+0.14r_t \tag{17}$$

Since $0\le r_t\le 1$, the controller keeps all parameters within finite intervals: $0.40\le\omega_t\le 0.90$, $1.10\le c_{1,\,t}, c_{2,\,t}\le 2.00$, $0.65\le p_{c,\,t}\le 0.95$, $0.02\le p_{m,\,t}\le 0.25$, and $0.02\le\sigma_{m,\,t}\le 0.16$.

3.4.5 Exploration, exploitation, and symmetry regulation

Normalized population diversity represents exploration. Search contraction represents exploitation:

$$E_t=d_t,\ X_t=1-E_t \tag{18}$$

The iteration-specific SRI is:

$$SRI_t=1-\frac{|E_t-X_t|}{E_t+X_t+\varepsilon} \tag{18}$$

The experiment aggregates iteration-specific values through temporal discounting:

$$SRI=\frac{\sum_{t=1}^{T}\lambda^{T-t}SRI_t}{\sum_{t=1}^{T}\lambda^{T-t}} \tag{19}$$

The mathematical basis of Equation (19) is the normalized exchange distance. Exchanging $(E_t,\ X_t)$ produces $(X_t,\ E_t)$, and $|E_t-X_t|$ measures departure from equality. Division by E_t+X_t normalizes this distance by the total magnitude of the two components, while subtraction from one converts distance into a symmetry score. The stabilization constant $\varepsilon=10^{-12}$ provides a numerical safeguard and has no substantive influence under Equation (18), where $E_t+X_t=1$. As ε approaches zero, Equation (19) reduces to twice the smaller component divided by the component sum. This limiting form lies in the unit interval, equals one under component equality, approaches zero as either component approaches zero, and remains unchanged after common positive rescaling. With $\varepsilon=10^{-12}$ and Equation (18), the implemented value differs from the limiting form by less than 10^{-12}. Exchange of the exploration and exploitation components leaves both forms unchanged. SRI therefore measures proportional equality within a normalized two-component search structure.

Because normalized exploration and exploitation sum

to one, the index equals twice the smaller component. Any score s represents a smaller component share of s/2, a larger component share of 1 − s/2, and an absolute dominance gap of 1 − s. A score of 0.60 represents a 0.30/0.70 split, whereas 0.20 represents a 0.10/0.90 split. Component trajectories identify whether exploration or exploitation dominates.

SRI implements exchange invariance, unit bounds, and a linear mapping of normalized absolute difference. Population diversity measures candidate dispersion [29], while allocation entropy captures concentration in the selected vector. Metaheuristic research treats exploration-exploitation balance as a central design concern [12]. For SRI validation, this study uses binary entropy and proportional balance as alternative representations of search balance. Together, these measures address related properties at different analytical levels. Exchange symmetry contributes a distinct representation of proportional equality when the normalized exploration and exploitation components exchange positions. A value of one denotes exact structural symmetry, and lower values indicate increasing proportional asymmetry. Component trajectories identify the direction of dominance. This formulation positions SRI as a structural diagnostic within the broader set of search measures.

Table 2 defines the symbols and parameters used throughout the mathematical formulation.

Table 2. Definition of symbols and parameters

Symbol	Definition	Operational role
n	Number of decision alternatives	Defines the allocation-vector dimension
m	Number of decision criteria	Defines the attribute and weight dimensions
$\mathrm{x}_{i,t}$	Position of candidate or particle i at iteration t	Represents a feasible decision allocation
Δ^{n-1}	Probability simplex	Defines nonnegative allocations with a unit sum
Π_{Δ}	Euclidean projection onto the simplex	Restores feasibility after each transition
A	Alternative-attribute matrix	Contains scores for the decision alternatives
w	Criterion-weight vector	Represents decision priorities
u	Weighted utility vector, Aw	Provides the linear utility component
R	Positive semidefinite risk matrix	Represents allocation risk dependence
ρ	Risk-aversion parameter	Controls the quadratic risk penalty
$F(\mathrm{x})$	Risk-adjusted objective function	Evaluates candidate decision quality
$\mathrm{y}_{i,t}$	GA offspring before mutation	Carries the crossover result
$\alpha_{i,t}$	Blend-crossover weight vector	Combines two parent solutions
$\mathrm{m}_{i,t}$	Bernoulli mutation-indicator vector	Selects mutated allocation components
$\eta_{i,t}$	Gaussian mutation vector	Perturbs selected components
$\mathrm{v}_{i,t}$	PSO velocity vector	Determines particle movement
$\mathrm{p}_{i,t}$	Personal-best position	Represents particle-level search memory
g_{t}	Global-best position	Represents population-level search memory
ω_t	Inertia weight	Controls velocity persistence
$c_{1,t}$	Cognitive coefficient	Controls attraction to personal best
$c_{2,t}$	Social coefficient	Controls attraction to global best
$p_{c,t}$	Crossover probability	Controls GA recombination frequency
$p_{m,t}$	Mutation probability	Controls mutation frequency
$\sigma_{m,t}$	Mutation scale	Controls mutation magnitude

a	Initial anchor vector	Defines the salient initial allocation
b	Bias strength	Controls cognitive-disturbance intensity
$\tilde{\mathbf{x}}_{i,t}$	Position after cognitive disturbance	Represents the bias-affected transition
D_t	Population diversity	Measures candidate dispersion
D_0	Initial population diversity	Normalizes candidate dispersion
q_t	Anchor concentration	Measures population proximity to the anchor
L_t	Consecutive stagnation count	Measures absence of objective improvement
d_t	Normalized diversity signal	Represents retained search dispersion
s_t	Normalized stagnation signal	Represents search stagnation
r_t	Exploration-demand signal	Governs MBIM parameter adjustment
E_t	Exploration ratio	Represents normalized population diversity
X_t	Exploitation ratio	Represents search contraction
SRI_t	Iteration-specific SRI	Measures proportional equality of exploration and exploitation
SRI	Temporally aggregated index	Summarizes symmetry across the complete trajectory
λ	Temporal discount factor	Controls the weight assigned to recent iterations
ε	Stabilization constant	Prevents division by zero
N	Population size	Defines the number of candidate solutions
T	Iteration limit	Defines the search horizon

3.5 Experimental design and evaluation metrics

Twelve stylized allocation scenarios comprised four instances of partner selection, four of investment prioritization, and four of opportunity assessment. Each instance applied the constrained allocation model in Equations (1)-(3) to ten alternatives and four normalized criteria. Application labels supplied analytical interpretations within a shared data-generating process. The common mathematical structure supported controlled comparison across search configurations. A beta distribution with shape parameters 2.2 and 2.0 generated the alternative attributes. Its support matches the unit scale of the criterion scores, while its mean of 0.524 creates mild input asymmetry without concentrating observations near either boundary. This asymmetry prevents an exactly symmetric input distribution from predetermining the symmetry assessment. A symmetric Dirichlet distribution with concentration parameter 2 generated the criterion weights. Equal concentration assigns every criterion the same expected weight, while a value of 2 permits variation across scenarios and limits single-criterion dominance. A normalized positive semidefinite matrix with maximum eigenvalue 1 represented correlated allocation risk. Risk aversion followed a uniform distribution on [0.08, 0.18]. For any feasible allocation, $x^{\top}Rx \leq 1$. The normalization limits the risk penalty to 0.18 and sets its scenario-specific upper bound within [0.08, 0.18] of the unit utility scale. The generator retained all ten alternatives and every attribute and risk relation, which defines complete sampling coverage as a controlled assumption.

An alternative from the lowest utility tercile supplied the anchor, which created a salient initial reference that competed with the unbiased objective. Bias strength b followed a uniform distribution on [0.35, 0.65]. One draw defined each scenario, and the resulting value remained fixed across iterations, paired replications, and search configurations. This interval produced moderate disturbances under the three implemented mechanisms: anchoring drift ranged from 0.01225 to 0.02275, confirmation resistance probability ranged from 0.1925 to 0.3575, and the overconfidence exponent ranged from 1.07 to 1.13. The initial population followed a Dirichlet distribution with base concentration 0.8 and an anchor increment of $5 + 12b$. Under the selected bias interval, the expected allocation share assigned to the anchor ranged from 0.581 to 0.654. This calibration created a measurable

bias-affected initial state while preserving allocation mass for the remaining alternatives.

All configurations used a population of 50 candidate solutions and an iteration limit of 500. The common computational budget isolated differences in search coordination from differences in available evaluations. The GA used tournament selection with three candidates, an elite count of two, a crossover probability of 0.90, a mutation probability of $1/n = 0.10$, and a mutation scale of 0.06. Evolutionary computation research provides the broader methodological basis for GA search design [14], while prior work demonstrates the integration of genetic and swarm operators within a hybrid optimizer [20]. The present study fixes the stated GA parameters across all relevant runs. The fixed GA-PSO configuration used an inertia weight of 0.70, equal cognitive and social coefficients of 1.50, and a velocity limit of 0.20. Equal learning coefficients avoided a prior preference for personal or social attraction, while the velocity limit restricted a single particle movement relative to the unit simplex. GA and PSO research documents the importance of hyperparameter configuration [21], while broader metaheuristic studies examine parameter tuning and algorithm performance across search methods [62, 63]. The present study fixes these PSO values to maintain a consistent configuration across comparative runs. The hybrid schedule applied five PSO transitions followed by a GA renewal of the half of the population with the lowest objective values. This renewal introduced population variation while preserving the other half of the swarm.

MBIM retained the same objective function, population, iteration budget, bias disturbance, and hybrid schedule. Equations (14)-(17) governed its parameter adjustments. Controller weights of 0.45, 0.30, and 0.25 assigned the largest contribution to diversity loss because it measures contraction of the search distribution, followed by stagnation and anchor concentration. Their unit sum bounded the exploration-demand signal. The parameter mappings included the fixed GA-PSO values within every adaptive interval and restricted all updates to the ranges established in Section 3.6. These values constitute a controlled baseline calibration that isolates search behavior; organizational data remain necessary for external validation.

One-factor-at-a-time sensitivity tests examined dependence on the baseline calibration. Alternative attribute distributions used Beta (2.0, 2.0) and Beta (2.6, 1.8); criterion-weight concentrations used 1 and 4; risk-aversion intervals used [0.04, 0.12] and [0.14, 0.24]; and bias-strength intervals used [0.20, 0.50] and [0.50, 0.80]. Controller tests assigned equal signal weights, stagnation-dominant weights (0.30, 0.45, 0.25), and bias-dominant weights (0.30, 0.25, 0.45). Population and swarm size tests used 30 and 70 candidates or particles against the baseline size of 50. Each condition retained the other calibration components, scenario identifiers, paired random seeds, and the 500-iteration budget. The analysis compared MBIM with fixed GA-PSO under 12 scenarios and 30 paired replications per scenario. Fourteen calibration conditions produced 10,080 model runs.

The main experiment applied 100 paired replications per scenario and held decision structure, bias exposure, and computational budgets constant under GA, fixed GA-PSO, and MBIM. Seed 638 defined the reproducible scenario and search sequences, producing 1,200 runs per configuration and 3,600 model runs. A projected-gradient procedure calculated the numerical reference allocation from a uniform starting point. The procedure used the step size $\frac{0.20}{\sqrt{k+1}}$, projected each update onto the simplex, and stopped when successive allocations differed by less than 10^{-11} or when the iteration count reached 10,000. Convergence time identified the first 20-iteration window in which every best-recorded objective value differed from the terminal value by at most 10^{-5}. Paired comparisons used 2,000 bootstrap samples to estimate 95% confidence intervals and paired standardized differences. Effect-size calculation divided the mean within-pair difference by the standard deviation of within-pair differences. A confidence interval excluding zero indicated configuration separation, while an interval containing zero supported a comparable-outcome interpretation.

SRI validation comprised 1,080 model runs across 12 scenarios, 30 replications, and three configurations. Scenario definitions, random seeds, population size, and 500 iterations matched the main experiment. Population diversity measured candidate dispersion [29]. Shannon entropy measured allocation concentration. Metaheuristic research treats exploration-exploitation balance as a central design concern [12]. This validation used binary exploration-exploitation entropy and proportional balance as alternative measures of search balance. Spearman correlations assessed SRI associations, 2,000 bootstrap samples estimated 95% confidence intervals, and discount factors of 0.95, 0.98, and 1.00 tested temporal sensitivity. Six metrics represented outcomes (DA and BRR), search structure (SRI and CS), and computational operation (AE and Adaptivity Index). The set combined established quality and convergence measures with bias correction, symmetry, stability, and adaptive control. Pooled and configuration-specific Spearman correlations assessed metric relationships; an absolute coefficient of 0.90 or greater indicated potential redundancy. Table 3 defines their operational forms.

Table 3. Evaluation metrics and operational definitions

Metric	Operational form	Interpretation
DA	$clip\left[1-\frac{F(\mathrm{x}^{ref})-F(\mathrm{x}_T)}{\max\{F(\mathrm{x}^{ref})-F(\mathrm{a}),\ \varepsilon\}},\ 0,\ 1\right]$	Final decision quality relative to the numerical reference and anchor
Bias Reduction Rate (BRR)	$clip\left[1-\frac{\left\|\mathrm{x}_T-\mathrm{x}^{ref}\right\|_2}{\max\left\{\left\|\mathrm{a}-\mathrm{x}^{ref}\right\|_2,\ \varepsilon\right\}},\ 0,\ 1\right]$	Movement from the anchor toward the numerical reference
SRI	Equation (20)	Temporal proportionality of exploration and exploitation
CS	$clip\left[1-\frac{SD(\Delta F_t)}{\max\{\max_t F_t-\min_t F_t,\ \varepsilon\}},\ 0,\ 1\right]$	Variation in the best-recorded objective increments
AE	$1/t_c$	Inverse of the convergence iteration
Adaptivity Index	$\frac{1}{T-1}\sum_{t=1}^{T-1}\left\|\theta_{t+1}-\theta_t\right\|_2$	Mean Euclidean change in the six-parameter vector across consecutive iterations; zero indicates fixed parameters

In Table 3, $clip[z,\ 0,\ 1]=\min\{1,\ \max\{0,\ z\}\}$, x^{ref} denotes the numerical reference allocation, x_T denotes the final best-recorded allocation, a denotes the anchor, F_t denotes the best-recorded objective value at iteration t, t_c denotes the convergence iteration, and θ_t contains the GA and PSO parameters at iteration t.

Adaptivity Index measures controller activity through changes in the six GA and PSO parameters. Its mathematical definition calculates the mean Euclidean change in the parameter vector across consecutive iterations. A zero value represents fixed parameter settings, and positive values capture the magnitude of controller-induced parameter adjustment.

3.6 Mathematical properties and convergence analysis

The feasible set Δ^{n-1} is nonempty, closed, and bounded, which makes it compact. The objective function $F(\mathrm{x})=\mathrm{u}^{\top}\mathrm{x}-\rho\mathrm{x}^{\top}\mathrm{Rx}$ is continuous on this set. Symmetry and positive semidefiniteness of R give

$$\nabla^2 F(\mathrm{x})=-2\rho\mathrm{R}\preceq 0 \tag{21}$$

Concavity and compactness guarantee the existence of a global maximizer. The scenario generator forms R from $\mathrm{BB}^{\top}$ and normalizes it by its largest eigenvalue, where B is a square matrix with independent Gaussian entries. The matrix $\mathrm{BB}^{\top}$ is positive definite with probability one. Since $\rho>0$, strict concavity gives a unique maximizer for each generated scenario.

The Karush-Kuhn-Tucker conditions characterize this maximizer. For the equality multiplier μ and nonnegativity multipliers v, an allocation x^* satisfies

$$\mathrm{u}-2\rho\mathrm{Rx}^*-\mu\mathrm{1}+v=0,\ \mathrm{1}^{\top}x^*=1,\ x^*\succeq 0,\ v\succeq 0,\ v_i x_i^*=0 \tag{22}$$

These conditions are necessary and sufficient because the objective is concave and the feasible constraints are affine. They provide the theoretical basis for the projected-gradient reference calculation used in Section 3.5.

Every GA, PSO, and cognitive-bias transition applies Euclidean projection to a proposed vector z:

$$\Pi_{\Delta}(\mathrm{z})=\underset{\mathrm{x}\in\Delta^{n-1}}{\operatorname{argmin}}\left\|\mathrm{x}-\mathrm{z}\right\|_2^2 \tag{23}$$

Projection preserves nonnegativity and the unit-sum constraint. Euclidean projection onto a closed convex set is nonexpansive, so

$$\left\|\Pi_{\Delta}(\mathrm{z})-\Pi_{\Delta}(\mathrm{y})\right\|_2\le\left\|\mathrm{z}-\mathrm{y}\right\|_2 \tag{24}$$

This property keeps every candidate feasible and prevents projection from amplifying the distance created by a search transition.

The controller inputs satisfy $0\le d_t,\ s_t,\ q_t\le 1$. The nonnegative signal weights in Equation (14) sum to one, which gives $0\le r_t\le 1$. Substitution into Equations (15)-(17) yields $0.40\le\omega_t\le 0.90$, $1.10\le c_{1,t},\ c_{2,t}\le 2.00$, $0.65\le p_{c,t}\le 0.95$, $0.02\le p_{m,t}\le 0.25$, and $0.02\le\sigma_{m,t}\le 0.16$. These intervals contain the fixed GA-PSO parameters and prevent unbounded controller output.

Let M_t denote the highest objective value retained through iteration t:

$$M_t = \max_{1 \le k \le t,\ 1 \le i \le N} F(\mathrm{x}_{i,k}) \tag{25}$$

Elitist retention and personal-best storage give

$$M_{t+1} = \max\left\{M_t,\ \max_{1 \le i \le N} F(\mathrm{x}_{i,t+1})\right\} \ge M_t \tag{26}$$

Continuity on the compact simplex supplies a finite upper bound F^*, so $M_t \le F^*$. The monotone convergence theorem therefore gives

$$\lim_{t \to \infty} M_t = \bar{M},\ \bar{M} \le F^* \tag{27}$$

This proof establishes convergence of the retained best-objective sequence under all three configurations. Its scope concerns objective-value convergence under bounded search parameters. Particle-wise convergence and certain attainment of the global maximizer require additional reachability assumptions beyond the claims evaluated in this study.

3.7 Validation and evaluation module

DSR treats artifact evaluation as a core stage of the research process [48, 49]. Venable et al. [58] propose the Framework for Evaluation in Design Science Research (FEDS), which classifies simulations and controlled experiments as forms of artificial evaluation. The present study evaluates the instantiated artifact through repeated computational experiments and comparative configuration analysis to assess the robustness of decision trajectories. The study applies identical scenario generation rules, iteration budgets, and random seeds in each experimental setting to ensure reproducibility. Repeated runs reveal whether configuration-specific behavioral profiles persist across different forms of cognitive distortion.

Comparator selection follows a nested configuration design. GA provides the evolutionary-search reference. Fixed GA-PSO adds swarm coordination while retaining constant parameters. MBIM retains the same GA-PSO operators and introduces bounded bias-responsive control. This sequence isolates the effects of hybridization and adaptive control. Adaptive GA, adaptive PSO, Differential Evolution, Covariance Matrix Adaptation Evolution Strategy (CMA-ES), and reinforcement learning-based optimization introduce different operators or learning formulations and address cross-algorithm optimization performance. Comparative claims concern the three nested configurations and the specified scenario space.

The fixed GA-PSO and MBIM comparison serves as a controller ablation because both configurations share the objective function, search operators, hybrid schedule, bias disturbances, population size, iteration budget, and paired random seeds. Their defining difference concerns the adaptive controller. Paired differences in outcome and process measures identify the behavioral changes associated with controller activation under the specified experimental conditions.

The evaluation module focuses on characterizing stability and structural differentiation in decision trajectories across configurations. Convergence behavior and trajectory patterns indicate whether configuration-specific behavioral profiles persist under controlled experimental settings. The SRI describes the exploration-exploitation relation as an empirical property of the decision process, enabling systematic comparison among GA, fixed GA-PSO, and MBIM.

Validation emphasizes robustness as the consistency of metric patterns and trajectory properties observed across repeated trials. MBIM provides a structural regulation mechanism that shapes decision dynamics under bias exposure, while the evaluation module supports systematic characterization and comparison through observable indicators derived from experimental outcomes. These procedures establish technical and analytical utility under controlled conditions. Organizational utility requires a subsequent naturalistic evaluation that uses expert assessment, user studies, historical decision records, or field implementation.

4. Results

Results identify distinct process profiles across GA, fixed GA-PSO, and MBIM under a common experimental design. All configurations achieve high DA, while fixed GA-PSO and MBIM record stronger bias reduction than GA. GA records the highest symmetry and stability, MBIM occupies an intermediate position, and fixed GA-PSO records the lowest values. Parameter adaptation distinguishes MBIM from both fixed configurations.

4.1 Output characteristics

All three configurations completed 1,200 runs and produced finite, feasible outputs. The retention mechanisms preserved the highest recorded objective value across iterations. Convergence timing differed across configurations.

Figure 2 presents representative convergence trajectories for GA, fixed GA-PSO, and MBIM.

The representative run shows that MBIM reaches its terminal objective value at iteration 9 and fixed GA-PSO at iteration 11. GA follows a gradual sequence of improvements and reaches a lower terminal value at iteration 411.

These trajectories characterize outcome convergence under a shared objective and bias disturbance. SRI, CS, AE, and adaptivity provide the corresponding process-level distinctions.

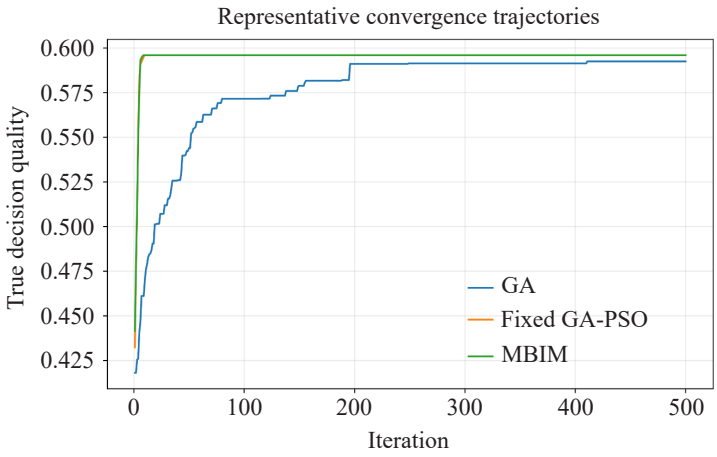


Figure 2. Representative convergence trajectories for the partner-selection scenario with anchoring bias (Scenario 1, replication 1, seed 638)

4.2 Metric-level performance

4.2.1 DA

DA averaged 0.965 for GA, 0.991 for fixed GA-PSO, and 0.991 for MBIM. Paired differences from GA reached 0.0263 for fixed GA-PSO and 0.0264 for MBIM. Bootstrap analysis produced 95% confidence intervals of [0.0235, 0.0292] for fixed GA-PSO minus GA and [0.0236, 0.0292] for MBIM minus GA. MBIM exceeded fixed GA-PSO by 0.00006; its confidence interval ranged from 0.00000 to 0.00013.

Fixed GA-PSO and MBIM achieved comparable practical accuracy. Their standardized paired difference of 0.050 indicates a small separation. Both hybrid configurations improved final solution quality relative to GA under the shared experimental conditions. DA evaluates outcome attainment, while process-level indicators assess search dynamics.

4.2.2 BRR

BRR averaged 0.909 for GA, 0.967 for fixed GA-PSO, and 0.968 for MBIM. Paired differences from GA reached 0.0583 for fixed GA-PSO and 0.0585 for MBIM. Bootstrap analysis produced 95% confidence intervals of [0.0528, 0.0638] for fixed GA-PSO minus GA and [0.0530, 0.0641] for MBIM minus GA. The MBIM minus fixed GA-PSO difference reached 0.0002, and its confidence interval included zero.

Fixed GA-PSO and MBIM achieved comparable bias contraction. Their standardized paired difference of 0.050 indicates a small separation. Comparable BRR values coexist with different symmetry profiles, which separates distortion contraction from exchange symmetry.

4.2.3 SRI

Mean SRI values followed this order: GA, 0.604; MBIM, 0.347; fixed GA-PSO, 0.162. Pairwise comparison yielded these differences: GA minus fixed GA-PSO, 0.4411; GA minus MBIM, 0.2567; MBIM minus fixed GA-PSO, 0.1845. Bootstrap analysis yielded these 95% confidence intervals: GA minus fixed GA-PSO, [0.4305, 0.4508]; GA minus MBIM, [0.2477, 0.2664]; MBIM minus fixed GA-PSO, [0.1809, 0.1881]. The standardized MBIM minus fixed GA-PSO difference reached 2.884.

These mean scores imply the following weighted minor-component shares: GA, 0.302; MBIM, 0.174; fixed GA-PSO, 0.081. Corresponding dominant shares reach 0.698, 0.826, and 0.919. Exploration and exploitation trajectories identify the dominant search function.

Rankings by SRI differ from those based on DA and BRR. GA records the highest symmetry with lower outcome and bias-reduction values. Fixed GA-PSO and MBIM achieve comparable DA and BRR, with MBIM recording higher symmetry. These patterns identify SRI as a descriptive structural indicator of search allocation. Performance evaluation requires separate consideration of DA, bias reduction, stability, efficiency, and adaptivity. Appropriate interpretation concerns the observed search structure and its relation to these complementary performance dimensions.

4.2.4 CS

Mean CS values followed this order: GA, 0.989; MBIM, 0.982; fixed GA-PSO, 0.981. Pairwise comparison yielded these differences: GA minus fixed GA-PSO, 0.0086; GA minus MBIM, 0.0077; MBIM minus fixed GA-PSO, 0.0009. Bootstrap analysis yielded these 95% confidence intervals: GA minus fixed GA-PSO, [0.0084, 0.0088]; GA minus MBIM, [0.0075, 0.0078]; MBIM minus fixed GA-PSO, [0.0009, 0.0010].

All configurations maintained high CS. GA recorded the highest value despite lower DA and BRR. MBIM exceeded fixed GA-PSO by 0.0009. Narrow dispersion in the paired differences produced a standardized difference of 0.906.

Stability captures trajectory consistency as a distinct process property.

4.2.5 Adaptivity Index

Adaptivity Index distinguished MBIM from the two fixed configurations. MBIM recorded a mean Adaptivity Index of 0.0587, while GA and fixed GA-PSO recorded zero because both retained constant parameters. Both MBIM contrasts produced a paired difference of 0.0587 and a standardized difference of 12.455. Confidence intervals covered [0.0585, 0.0590] against GA and [0.0584, 0.0590] against fixed GA-PSO.

MBIM adjusted six GA and PSO parameters in response to the controller signals. GA and fixed GA-PSO retained their specified values during the runs. Comparable DA and BRR values for MBIM and fixed GA-PSO indicate that Adaptivity Index captures parameter activity as a process property.

4.2.6 AE

Hybrid search produced the main efficiency advantage. Mean AE followed this order: fixed GA-PSO, 0.0787; MBIM, 0.0738; GA, 0.0084. Confidence intervals confirmed both hybrid contrasts: fixed GA-PSO minus GA, [0.0684, 0.0720]; MBIM minus GA, [0.0638, 0.0670]. Fixed GA-PSO exceeded MBIM by 0.0049, with a confidence interval of [0.0038, 0.0060].

Both hybrid configurations achieved greater efficiency than GA. Fixed GA-PSO held a modest advantage over MBIM, and their standardized paired difference reached 0.246. MBIM recorded higher SRI and CS with a lower AE than fixed GA-PSO. AE captures convergence speed and complements the outcome and structural indicators.

Table 4 reports the metric values used in the analysis.

Table 4. Main experiment metric values across search configurations

Search configuration	DA	SRI	CS	AE	BRR	Adaptivity Index*
GA	0.965	0.604	0.989	0.0084	0.909	0.0000
Fixed GA-PSO	0.991	0.162	0.981	0.0787	0.967	0.0000
MBIM	0.991	0.347	0.982	0.0738	0.968	0.0587

*GA and fixed GA-PSO retain fixed parameters and record Adaptivity Index = 0. MBIM adjusts its parameters through the adaptive controller and records Adaptivity Index = 0.0587.

4.3 Cross-module behavioral interpretation

MBIM combines outcome attainment with adaptive search control. It recorded DA = 0.991, BRR = 0.968, SRI = 0.347, and Adaptivity Index = 0.0587. This profile couples strong correction with intermediate symmetry and active parameter adjustment.

Fixed GA-PSO emphasizes outcome correction and efficiency. It recorded DA = 0.991, BRR = 0.967, AE = 0.0787, and SRI = 0.162. Fixed hybrid coordination combines strong correction and the highest efficiency with the lowest symmetry.

Table 5. Behavioral profiles of search configurations under biased evaluation

Search configuration	Behavioral orientation	Structural pattern	Bias response mode	Stability and efficiency profile
GA	Symmetry and stability	High symmetry with fixed evolutionary search	Moderate bias contraction	Highest stability; lowest efficiency
Fixed GA-PSO	Efficiency and outcome correction	Low symmetry with fixed hybrid search	Strong bias contraction	High stability; highest efficiency
MBIM	Adaptive integration	Intermediate symmetry with adaptive hybrid search	Strong bias contraction	High stability and efficiency; active parameter control

*Behavioral profiles synthesize Table 4 metrics and Section 4.3 interpretations. Each profile identifies a dominant process orientation. Performance assessment requires joint consideration of outcome, symmetry, stability, efficiency, bias reduction, and adaptation.

GA forms a distinct profile. It recorded SRI = 0.604 and CS = 0.989, leading the three configurations on both measures, while DA = 0.965, BRR = 0.909, and AE = 0.0084 fell below the hybrid values. Gradual convergence combines symmetry and stability with lower outcome correction and efficiency.

These profiles show that symmetry, accuracy, bias reduction, stability, efficiency, and adaptation represent distinct performance dimensions. A configuration can lead on one dimension and occupy a different position on another.

Table 5 presents the behavioral profiles derived from the cross-module interpretation.

4.4 Comparative performance synthesis

Comparison of GA with fixed GA-PSO isolates hybrid coordination. Fixed GA-PSO produced DA, BRR, and AE gains of 0.0263, 0.0583, and 0.0702. GA retained higher SRI and CS; the gaps reached 0.4411 and 0.0086. These contrasts show that fixed hybrid coordination strengthens outcome correction and efficiency while reducing symmetry and stability.

MBIM and fixed GA-PSO provide a controller ablation test. Both configurations share the hybrid operators, objective function, bias disturbances, computational budget, and paired random seeds. Controller activation increases SRI by 0.1845, CS by 0.0009, and Adaptivity Index by 0.0587. DA and BRR show comparable values, while fixed GA-PSO retains a 0.0049 AE advantage. These results link adaptive control to changes in symmetry, stability, and parameter activity while preserving DA and bias reduction.

The comparative synthesis concerns GA, fixed GA-PSO, and MBIM within the specified scenario space. Its claims address mechanism-level process regulation. These patterns clarify how structural properties shape decision behavior under biased evaluation without reliance on accuracy differences alone.

4.5 Sensitivity, robustness, and SRI validation

4.5.1 Calibration sensitivity and pattern robustness

All 14 calibration conditions produced positive MBIM minus fixed GA-PSO differences for SRI, CS, and Adaptivity Index. SRI differences ranged from 0.1082 to 0.2112, CS differences ranged from 0.0008 to 0.0012, and Adaptivity Index differences ranged from 0.0279 to 0.0638. All 95% bootstrap confidence intervals for these metrics excluded zero. AE differences ranged from −0.0103 to −0.0034, and every interval fell below zero. Adaptive control produced greater symmetry, stronger CS, persistent parameter activity, and a consistent efficiency cost under every calibration.

The [0.20, 0.50] bias-strength interval produced SRI and Adaptivity Index differences of 0.1867 and 0.0542. Higher bias strength under [0.50, 0.80] produced corresponding differences of 0.1754 and 0.0638. Confidence intervals for all four differences excluded zero.

DA differences ranged from 0.0000 to 0.0008, and BRR differences ranged from 0.0000 to 0.0093. Most confidence intervals included zero; the remaining intervals indicated small MBIM gains under selected conditions. The main outcome profile persisted in every calibration, as fixed GA-PSO and MBIM produced comparable decision quality and bias reduction.

Controller-weight changes produced the largest reductions in the SRI and Adaptivity Index effects. Bias-dominant weights reduced the SRI difference to 0.1082 and the Adaptivity Index difference to 0.0279, but both values stayed positive. Risk-high calibration increased the SRI difference to 0.2112, and bias-high calibration increased the Adaptivity Index difference to 0.0638. Difference-in-differences estimates showed changes in effect magnitude and preserved the baseline directions for SRI, CS, AE, and Adaptivity Index.

Table 6. Calibration sensitivity and pattern robustness

Metric	Baseline paired difference	Minimum	Maximum	Pattern under 14 conditions
DA	0.0000	0.0000	0.0008	Comparable accuracy with small MBIM gains
BRR	0.0000	0.0000	0.0093	Comparable bias reduction with small MBIM gains
SRI	0.1839	0.1082	0.2112	Positive under all conditions
CS	0.0009	0.0008	0.0012	Positive under all conditions
AE	−0.0044	−0.0103	−0.0034	Negative under all conditions
Adaptivity Index	0.0587	0.0279	0.0638	Positive under all conditions

Note: Values represent paired MBIM minus fixed GA-PSO differences. Positive SRI, CS, and Adaptivity Index values indicate higher MBIM values. Negative AE values indicate lower MBIM efficiency. All confidence intervals for SRI, CS, AE, and Adaptivity Index excluded zero. Complete confidence intervals and difference-in-differences estimates appear in the supplementary material.

Population and swarm size produced limited change in the SRI effect. Size 30 yielded an MBIM minus fixed GA-PSO SRI difference of 0.1822, size 50 yielded 0.1839, and size 70 yielded 0.1844. Difference-in-differences estimates relative to the size-50 baseline reached −0.0017 for size 30 and 0.0005 for size 70; their 95% confidence intervals were [−0.0048, 0.0014] and [−0.0019, 0.0027]. Both intervals included zero. Adaptivity Index differences reached 0.0602 at size 30, 0.0587 at size 50, and 0.0582 at size 70. These values show that adaptive activity remained positive while its magnitude displayed scale sensitivity. Table 6 summarizes the baseline estimates and full ranges; the supplementary material reports all condition-level results.

4.5.2 SRI validation and temporal sensitivity

SRI validation comprised 1,080 model runs. The design combined 12 scenarios, 30 paired replications per scenario, and three search configurations. A discount factor of 0.98 yielded these Spearman correlations with SRI: binary exploration-exploitation entropy, 0.9877; proportional balance ratio, 0.9959; raw population diversity, 0.9781; and best-allocation entropy, 0.6480. The three correlations above 0.97 confirm consistent rankings for search balance and dispersion. A weaker association with best-allocation entropy shows that exchange symmetry and allocation concentration capture related but distinct analytical properties.

Mean SRI reached 0.6137 for GA, 0.1619 for fixed GA-PSO, and 0.3457 for MBIM. MBIM exceeded fixed GA-PSO by 0.1839, with a 95% bootstrap confidence interval of [0.1771, 0.1903]. All 360 paired observations recorded a positive SRI difference. Binary entropy, proportional balance, and population diversity produced the same directional result. Best-allocation entropy yielded a mean paired difference of −0.00002, with a 95% confidence interval of [−0.00007, 0.00000]. Adaptive parameter control therefore changed the exploration-exploitation structure while preserving the concentration profile of the best allocation. Temporal discounting preserved the configuration order at 0.95, 0.98, and 1.00. GA ranked first under all three settings, MBIM ranked second, and fixed GA-PSO ranked third. Pairwise Spearman coefficients ranged from 0.9488 to 0.9966 and supported temporal stability. Table 7 reports the indicator comparisons and temporal sensitivity results.

Table 7. SRI validation and temporal sensitivity results

Panel A. Indicator comparison at a discount factor of 0.98				
Indicator	**GA**	**Fixed GA-PSO**	**MBIM**	**Spearman's rho with SRI**
SRI	0.6137	0.1619	0.3457	-
Binary exploration-exploitation entropy	0.8326	0.3540	0.5586	0.9877
Proportional balance ratio	0.4929	0.0955	0.2481	0.9959
Raw population diversity	0.0308	0.0064	0.0148	0.9781
Best-allocation entropy	0.3398	0.2232	0.2232	0.6480
Panel B. SRI sensitivity to temporal discounting				
Discount factor	**GA**	**Fixed GA-PSO**	**MBIM**	
0.95	0.6125	0.1638	0.3511	
0.98	0.6137	0.1619	0.3457	
1.00	0.6511	0.1782	0.3515	

Note: Spearman coefficients use all 1,080 model runs. Higher SRI, binary entropy, and proportional balance indicate greater exploration-exploitation symmetry. Population diversity measures candidate dispersion, while best-allocation entropy measures allocation concentration.

4.5.3 Metric relationships and redundancy

CS and AE produced the largest pooled absolute Spearman correlation, −0.7507. DA and BRR followed at 0.7072. SRI showed coefficients of −0.6491 with AE, −0.6261 with BRR, −0.5592 with DA, and 0.4347 with CS. Configuration analysis identified BRR and SRI as the strongest pair under GA at −0.8448, DA and SRI under fixed GA-PSO at −0.7786, and BRR and SRI under MBIM at −0.7239. Constant Adaptivity Index values prevented configuration-level estimates for GA and fixed GA-PSO. MBIM yielded absolute Adaptivity Index correlations from 0.0240 to 0.2928. Every eligible coefficient fell below the 0.90 threshold and satisfied the prespecified distinction criterion. Results support related but distinct roles for outcome, search structure, and computational operation

metrics. Supplementary Material reports the complete pooled and configuration-specific matrices.

5. Discussion

5.1 Interpretation of core results

Bias intervention in the present decision model operates through structural adjustment of search behavior. Fixed GA-PSO and MBIM achieved comparable DA and bias reduction, yet their SRI and Adaptivity Index values differed. This contrast separates outcome correction, symmetry regulation, and adaptive parameter control.

The contrasting profiles connect search structure, parameter control, and outcome performance and answer the research question. Metric relationships support distinct roles for outcome, search structure, and computational operation measures.

Validation results clarify the measurement role of SRI. Strong associations with binary entropy, proportional balance, and population diversity demonstrate convergence among measures of exploration-exploitation structure. Normalized diversity operationalizes exploration, which explains its association with population diversity. The lower association with best-allocation entropy and the near-zero difference across MBIM and fixed GA-PSO distinguish allocation concentration from exchange symmetry. SRI therefore represents a structural diagnostic rather than a general performance ranking. A complete interpretation of decision behavior combines SRI with DA, bias reduction, CS, AE, and adaptivity. Exploration and exploitation values identify the direction of dominance because exchange invariance assigns the same SRI to equal proportional imbalances in opposite directions.

5.2 Illustrative application to business development decisions

Structural patterns in the simulation provide analytical analogues for three business development tasks. Partner selection treats candidate firms as alternatives, commitment shares as allocation variables, and strategic fit, capability complementarity, governance readiness, and collaboration quality as criteria. Investment prioritization treats projects as alternatives, resource shares as allocation variables, and return potential, strategic fit, execution feasibility, and resource compatibility as criteria. Opportunity assessment treats markets or initiatives as alternatives, evaluation effort as the allocation variable, and market attractiveness, capability fit, timing readiness, and implementation feasibility as criteria. A salient initial option supplies the anchor in every mapping.

Within these mappings, population diversity represents the breadth of the candidate set, anchor concentration captures adherence to an initial preference, and SRI measures exploration-exploitation symmetry. MBIM recorded SRI = 0.347, DA = 0.991, BRR = 0.968, and CS = 0.982. Fixed GA-PSO produced lower symmetry, SRI = 0.162, with comparable DA and BRR but lower CS. GA produced higher symmetry, SRI = 0.604, with lower DA and BRR. These profiles show why SRI functions as a process diagnostic and requires joint interpretation with outcome and stability measures.

Organizational evaluation requires calibration through decision criteria, historical logs, expert judgments, and observed outcomes. Such evaluation can examine whether the resulting trajectories capture search contraction, adherence to an initial preference, and changes in symmetry. Field studies can test whether these indicators identify commitment imbalance and improve intervention timing or decision quality. The present evidence establishes an application mapping and an implementation specification; organizational evidence will determine managerial usefulness.

5.3 Adaptivity and design science implications

From a design science perspective, MBIM functions as a behavioral computational artifact that embeds rationality and control assumptions. SRI operates as a diagnostic signal of exploration-exploitation symmetry, while Adaptivity Index records controller-induced parameter changes that regulate search imbalance. MBIM's mean Adaptivity Index of 0.0587 documents parameter adjustment during execution; zero values for GA and fixed GA-PSO reflect their fixed specifications. This distinction separates adaptive control from symmetry assessment and outcome performance.

This design logic supplies a testable decision-support specification. Organizations can record diversity, anchor concentration, parameter changes, SRI, CS, and bias reduction during repeated evaluation. Comparison with managerial judgments and observed outcomes can determine whether these indicators detect commitment imbalance and support intervention.

Current evidence establishes the artifact's technical and analytical behavior under controlled conditions. Practical evaluation requires expert assessment and user interaction to examine interpretability, usability, and intervention timing. Organizational evaluation requires historical decision records and field implementation to assess decision quality and contextual fit. These evaluation stages extend the present computational assessment toward practical and organizational validation.

5.4 Theoretical and managerial implications

Exchange symmetry functions in this study as a measurable structural property of algorithmic decision processes. Cognitive bias reshapes exploration-exploitation allocation, while CS and parameter adaptation describe distinct features of the resulting search trajectory. This

perspective provides a computational representation of bias-induced changes in search allocation as observable properties of search structure.

The design science contribution arises from an executable artifact that integrates bias-responsive parameter control, symmetry assessment, and process-level diagnosis within an established GA-PSO architecture. Population diversity, search stagnation, and anchor concentration trigger bounded changes in search parameters. SRI and complementary indicators characterize the resulting decision trajectories. Algorithmic novelty resides in the artifact configuration and analytical use of adaptive search control. Established GA and PSO operators provide the computational foundation.

The framework proposes a managerial diagnostic logic for field evaluation. Decision teams can define alternatives, criteria, risk estimates, and the salient initial option. MBIM can monitor SRI, CS, and bias reduction during staged evaluation. Declining symmetry under stable convergence indicates search concentration, while reduced stability indicates an unsettled trajectory. Historical decision logs and observed outcomes must determine whether these signals improve intervention timing or decision quality.

This study contributes to the literature in three respects. First, it conceptualizes bias intervention as structural regulation within algorithmic decision processes. Second, it develops a decision-analysis artifact that integrates bias characterization, established GA-PSO search, configuration control, and process-level assessment of bias-affected decision dynamics. Third, it specifies complementary indicators that distinguish search structure, stability, bias reduction, adaptivity, and efficiency from DA.

Controlled simulation isolates structural dynamics under fixed bias conditions and permits direct comparison among search configurations. This design establishes computational behavior within the specified scenario space. The resulting evidence supports technical and analytical evaluation of the artifact under controlled conditions. Real organizational decisions incorporate social interaction, institutional constraints, changing criteria, and outcome feedback. Empirical validation requires decision data that connect the simulated mechanisms and indicators to observed organizational processes and outcomes. Parameter settings in the present study represent stylized decision environments.

Sampling bias can precede search-stage bias by changing the alternatives, attributes, and relationships available to the artifact. Shang [67] shows that uniform and nonuniform missing-data processes can produce different estimates of network robustness because topology, sampling method, attack mode, and missing-data level shape the observed subgraph. This insight implies that underrepresentation of partner types, projects, markets, or interdependencies can alter the candidate set, criterion matrix, and risk structure received by MBIM. The present simulation fixes sampling coverage and supports conclusions conditional on its data-generation assumptions. Future experiments can introduce uniform omission, nonuniform omission, selection bias, and corrupted relationship data to evaluate the persistence of the reported configuration profiles.

The calibration analysis varied population and swarm size, attribute distributions, criterion concentration, risk aversion, bias strength, and controller weights. Paired seeds and a common initialization rule controlled the initial search states. MBIM treated crossover and mutation probabilities as controller-regulated parameters, while fixed GA-PSO retained its baseline settings as the experimental control. Classical benchmark functions assess cross-algorithm optimization generalizability; the present evaluation examines a decision-analysis artifact across controlled allocation landscapes.

Practical validation requires historical decision logs, expert-calibrated criteria, and observed outcomes from partner selection, investment prioritization, or opportunity assessment. Such evidence can test predictive validity, contextual calibration, and managerial usefulness. Future research can test cross-algorithm generalizability by benchmarking MBIM against adaptive GA, adaptive PSO, Differential Evolution, CMA-ES, and reinforcement learning-based optimization.

6. Conclusion

This study develops the MBIM to examine bias-affected search dynamics in controlled simulations. Results show that MBIM maintains DA and bias reduction comparable to fixed GA-PSO while producing higher SRI and CS. MBIM's positive Adaptivity Index documents controller-induced parameter adjustment during execution, and decision quality requires joint interpretation of adaptivity, symmetry, stability, and outcome attainment. Exchange symmetry provides the study's theoretical framing. SRI expresses equality in normalized exploration and exploitation as a measurable search property. Computational results show how cognitive bias changes this property across simulated allocation scenarios. The conceptual contribution applies exchange symmetry to exploration-exploitation dynamics and operationalizes symmetry departure through SRI. MBIM supplies an executable setting that examines how bounded parameter control changes this structure under cognitive bias. Results support this computational interpretation across the tested scenarios and calibration conditions.

From a design science perspective, MBIM embeds behavioral assumptions in an executable computational artifact and makes bias regulation observable at the process level. Structural indicators support evaluation of search behavior beyond outcome accuracy. The design science contribution resides in artifact construction, executable specification, and technical evaluation. Controlled computational experiments provide technical and analytical evidence within the specified scenario space. Organizational evaluation requires representative

sampling, heterogeneous agents, stochastic signals, delayed feedback, historical decision records, and observed outcomes. Such evidence can assess contextual calibration, managerial usefulness, and theoretical generalizability.

Abbreviations

AE: Algorithmic Efficiency
BRR: Bias Reduction Rate
CMA-ES: Covariance Matrix Adaptation Evolution Strategy
CS: Convergence Stability
DA: Decision Accuracy
DSR: Design Science Research
GA: Genetic Algorithm
GA-PSO: Genetic Algorithm-Particle Swarm Optimization
MBIM: Metaheuristic-Based Bias Intervention Module
PSO: Particle Swarm Optimization
SRI: Symmetry Regulation Index

Declaration of generative AI use

The author declares that generative artificial intelligence (AI) tools were used during the preparation of this manuscript. AI use was limited to language improvement and translation. All AI-assisted outputs were reviewed, verified, and revised by the author. Generative AI was not used to replace the author's scientific judgment, generate unsupported scientific claims, interpret results independently, or assume responsibility for any part of the research. The author remains fully responsible for the originality, accuracy, integrity, and ethical compliance of the manuscript.

Funding

The author received no funding for this research.

Data availability

The datasets generated and analyzed during the current study are available in the electronic supplementary material. Source code for the MBIM, GA, and fixed GA-PSO models was submitted to the journal with the manuscript and is available from the corresponding author upon reasonable request.

Conflict of interest

The author reports no conflict of interest.

References

[1] Kurdoglu RS, Ates NY, Lerner DA. Decision-making under extreme uncertainty: Eristic rather than heuristic. *International Journal of Entrepreneurial Behavior & Research*. 2023; 29(3): 763-782. doi:10.1108/IJEBR-07-2022-0587.

[2] Berthet V. The impact of cognitive biases on professionals' decision-making: A review of four occupational areas. *Frontiers in Psychology*. 2022; 12: 802439. doi:10.3389/fpsyg.2021.802439.

[3] Cai Z, Yang X, Zhou M, Zhan ZH, Gao S. Toward explicit control between exploration and exploitation in evolutionary algorithms: A case study of differential evolution. *Information Sciences*. 2023; 649: 119656. doi:10.1016/j.ins.2023.119656.

[4] Gomroki G, Behzadi H, Fattahi R, Salehi Fadardi J. Identifying effective cognitive biases in information retrieval. *Journal of Information Science*. 2023; 49(3): 348-358. doi:10.1177/01655515211001777.

[5] Pittenger LM, Glassman AM, Mumbower S, Merritt DM, Bollenback D. Bounded rationality: Managerial decision-making and data. *Journal of Computer Information Systems*. 2023; 63(4): 890-903. doi:10.1080/08874417.2022.2111380.

[6] Wang Y, Luan S, Gigerenzer G. Modeling fast-and-frugal heuristics. *PsyCh Journal*. 2022; 11(4): 600-611. doi:10.1002/pchj.576.

[7] Hodgkinson GP, Burkhard B, Foss NJ, Grichnik D, Sarala RM, Tang Y, et al. The heuristics and biases of top managers: Past, present, and future. *Journal of Management Studies*. 2023; 60(5): 1033-1063. doi:10.1111/joms.12937.

[8] Bailey DE, Faraj S, Hinds PJ, Leonardi PM, von Krogh G. We are all theorists of technology now: A relational perspective on emerging technology and organizing. *Organization Science*. 2022; 33(1): 1-18. doi:10.1287/orsc.2021.1562.

[9] Parent-Rocheleau X, Parker SK. Algorithms as work designers: How algorithmic management influences the design of jobs. *Human Resource Management Review*. 2022; 32(3): 100838. doi:10.1016/j.hrmr.2021.100838.

[10] Ashby WR. Requisite variety and its implications for the control of complex systems. In: Klir GJ. (ed.) *Facets of Systems Science*. Boston (MA): Springer; 1991. p.405-417. doi:10.1007/978-1-4899-0718-9_28.

[11] March-Pons D, Pastor-Satorras R, Miguel MC. Symmetry breaking in collective decision-making through higher-order interactions. *npj Complexity*. 2026; 3(1): 7. doi:10.1038/s44260-026-00071-5.

[12] Lazo Y, Crawford B, Cisternas-Caneo F, Barrera-Garcia J, Soto R, Giachetti G. Evolution and trends of the exploration-exploitation balance in bio-inspired optimization algorithms: A bibliometric analysis of metaheuristics. *Biomimetics*. 2025; 10(8): 517. doi:10.3390/biomimetics10080517.

[13] Rajwar K, Deep K, Das S. An exhaustive review of the metaheuristic algorithms for search and optimization: Taxonomy, applications, and open challenges. *Artificial Intelligence Review*. 2023; 56(11): 13187-13257. doi:10.1007/s10462-023-10470-y.

[14] Zhan ZH, Shi L, Tan KC, Zhang J. A survey on evolutionary computation for complex continuous optimization. *Artificial Intelligence Review*. 2022; 55(1): 59-110. doi:10.1007/s10462-021-10042-y.

[15] Jami A, Abbaszade S, Vahabie AH. A review on exploration-exploitation trade-off in psychiatric disorders. *BMC Psychiatry*. 2025; 25: 420. doi:10.1186/s12888-025-06837-w.

[16] Wilson RC, Bonawitz E, Costa VD, Ebitz RB. Balancing exploration and exploitation with information and randomization. *Current Opinion in Behavioral Sciences*. 2021; 38: 49-56. doi:10.1016/j.cobeha.2020.10.001.

[17] Park S, Puranam P. Self-confirming biased beliefs in organizational 'learning by doing'. *Complexity*. 2021; 2021: 8865872. doi:10.1155/2021/8865872.

[18] Kasper J, Fiedler K, Kutzner F, Harris CA. On the role of exploitation and exploration strategies in the maintenance of cognitive biases: Beyond the pursuit of instrumental rewards. *Memory & Cognition*. 2023; 51(6): 1374-1387. doi:10.3758/s13421-023-01393-8.

[19] Schatzki L, Larocca M, Nguyen QT, Sauvage F, Cerezo M. Theoretical guarantees for permutation-equivariant quantum neural networks. *npj Quantum Information*. 2024; 10: 12. doi:10.1038/s41534-024-00804-1.

[20] Awad A, Hawash A, Abdalhaq B. A genetic algorithm and swarm-based binary decision diagram reordering optimizer reinforced with recent operators. *IEEE Transactions on Evolutionary Computation*. 2023; 27(3): 535-549. doi:10.1109/TEVC.2022.3170212.

[21] Papazoglou G, Biskas P. Review and comparison of genetic algorithm and particle swarm optimization in the optimal power flow problem. *Energies*. 2023; 16(3): 1152. doi:10.3390/en16031152.

[22] Solano-Rojas BJ, Villalón-Fonseca R, Batres R. Micro evolutionary particle swarm optimization (MEPSO): A new modified metaheuristic. *Systems and Soft Computing*. 2023; 5: 200057. doi:10.1016/j.sasc.2023.200057.

[23] Hadj Slama A, Saidi L, Saidi M, Benbouzid M. Metaheuristic optimization of hybrid renewable energy systems under asymmetric cost-reliability objectives: NSGA-II and MOPSO approaches. *Symmetry*. 2025; 17(9): 1412. doi:10.3390/sym17091412.

[24] Hevner AR, March ST, Park J, Ram S. Design science in information systems research. *MIS Quarterly*. 2004; 28(1): 75-105. doi:10.2307/25148625.

[25] De Sordi JO. *Design Science Research Methodology: Theory Development from Artifacts*. Cham: Palgrave Macmillan; 2021. doi:10.1007/978-3-030-82156-2.

[26] Boussaïd I, Lepagnot J, Siarry P. A survey on optimization metaheuristics. *Information Sciences*. 2013; 237: 82-117. doi:10.1016/j.ins.2013.02.041.

[27] Holland JH. Studying complex adaptive systems. *Journal of Systems Science and Complexity*. 2006; 19(1): 1-8. doi:10.1007/s11424-006-0001-z.

[28] Bolufé-Röhler A, Tamayo-Vera D. Machine learning for enhancing metaheuristics in global optimization: A comprehensive review. *Mathematics*. 2025; 13(18): 2909. doi:10.3390/math13182909.

[29] Osuna-Enciso V, Cuevas E, Castañeda BM. A diversity metric for population-based metaheuristic algorithms. *Information Sciences*. 2022; 586: 192-208. doi:10.1016/j.ins.2021.11.073.

[30] Sheldrick RC, Cruden G, Schaefer AJ, Mackie TI. Rapid-cycle systems modeling to support evidence-informed decision-making during system-wide implementation. *Implementation Science Communications*. 2021; 2(1): 116. doi:10.1186/s43058-021-00218-6.

[31] McGrath RG. Who learns fastest, wins: Lean startup and discovery driven growth. *Journal of Management*. 2024; 50(8): 3162-3182. doi:10.1177/01492063231204870.

[32] Cohen JD, McClure SM, Yu AJ. Should I stay or should I go? How the human brain manages the trade-off between exploitation and exploration. *Philosophical Transactions of the Royal Society B: Biological Sciences*. 2007; 362(1481): 933-942. doi:10.1098/rstb.2007.2098.

[33] Flyvbjerg B. Top ten behavioral biases in project management: An overview. *Project Management Journal*. 2021; 52(6): 531-546. doi:10.1177/87569728211049046.

[34] Ahmed BS. An adaptive metaheuristic framework for changing environments. In: *Proceedings of the 2024 IEEE Congress on Evolutionary Computation (CEC)*. Yokohama, Japan. Piscataway (NJ): IEEE; 2024. p.1-10. doi:10.1109/CEC60901.2024.10611806.

[35] Wang S, Qiao P, Yue Q, Xu Z, Shang Q. Research on dynamic particle swarm optimization for multi-objective reconnaissance task allocation of UAVs. *Drones*. 2025; 9(8): 556. doi:10.3390/drones9080556.

[36] Gavetti G. Perspective—Toward a behavioral theory of strategy. *Organization Science*. 2012; 23(1): 267-285. doi:10.1287/orsc.1110.0644.

[37] Audia PG, Brion S. Reluctant to change: Self-enhancing responses to diverging performance measures. *Organizational Behavior and Human Decision Processes*. 2007; 102(2): 255-269. doi:10.1016/j.obhdp.2006.01.007.

[38] Nickerson RS. Confirmation bias: A ubiquitous phenomenon in many guises. *Review of General Psychology*. 1998; 2(2): 175-220. doi:10.1037/1089-2680.2.2.175.

[39] Bastian B, Acar OA, Boom H, Smits J. Management decisions under radical uncertainty. *Management Decision*. 2025; 63(13): 714-729. doi:10.1108/MD-

01-2025-0079.
[40] Geng X, Zhao Y, Xu S, Sun X, Zhou X. Group collaboration reduces delay discounting of intertemporal choices and its duration. *Judgment and Decision Making*. 2024; 19: e34. doi:10.1017/jdm.2024.20.
[41] Fasolo B, Heard C, Scopelliti I. Mitigating cognitive bias to improve organizational decisions: An integrative review, framework, and research agenda. *Journal of Management*. 2025; 51(6): 2182-2211. doi:10.1177/01492063241287188.
[42] Yukalov VI. Systems with symmetry breaking and restoration. *Symmetry*. 2010; 2(1): 40-68. doi:10.3390/sym2010040.
[43] Swan J, Adriaensen S, Brownlee AE, Hammond K, Johnson CG, Kheiri A, et al. Metaheuristics 'in the large'. *European Journal of Operational Research*. 2022; 297(2): 393-406. doi:10.1016/j.ejor.2021.05.042.
[44] Dorigo M, Gambardella LM. Ant colony system: A cooperative learning approach to the traveling salesman problem. *IEEE Transactions on Evolutionary Computation*. 1997; 1(1): 53-66. doi:10.1109/4235.585892.
[45] Rashedi E, Nezamabadi-Pour H, Saryazdi S. GSA: A gravitational search algorithm. *Information Sciences*. 2009; 179(13): 2232-2248. doi:10.1016/j.ins.2009.03.004.
[46] Yang XS. Firefly algorithms for multimodal optimization. In: Watanabe O, Zeugmann T. (eds.) *Stochastic Algorithms: Foundations and Applications*. Berlin: Springer; 2009. p.169-178. doi:10.1007/978-3-642-04944-6_14.
[47] Karakatič S, Podgorelec V. A survey of genetic algorithms for solving multi-depot vehicle routing problem. *Applied Soft Computing*. 2015; 27: 519-532. doi:10.1016/j.asoc.2014.11.005.
[48] Gregor S, Hevner AR. Positioning and presenting design science research for maximum impact. *MIS Quarterly*. 2013; 37(2): 337-355. doi:10.25300/MISQ/2013/37.2.01.
[49] Peffers K, Tuunanen T, Rothenberger MA, Chatterjee S. A design science research methodology for information systems research. *Journal of Management Information Systems*. 2007; 24(3): 45-77. doi:10.2753/MIS0742-1222240302.
[50] van der Aalst WMP, Bichler M, Heinzl A. Responsible data science. *Business & Information Systems Engineering*. 2017; 59(5): 311-313. doi:10.1007/s12599-017-0487-z.
[51] Mehrabi N, Morstatter F, Saxena N, Lerman K, Galstyan A. A survey on bias and fairness in machine learning. *ACM Computing Surveys*. 2021; 54(6): 1-35. doi:10.1145/3457607.
[52] Kuechler W, Vaishnavi V. A framework for theory development in design science research: Multiple perspectives. *Journal of the Association for Information Systems*. 2012; 13(6): 395-423. doi:10.17705/1jais.00300.
[53] vom Brocke J, Hevner A, Maedche A. Introduction to design science research. In: vom Brocke J, Hevner A, Maedche A. (eds.) *Design Science Research: Cases*. Cham: Springer; 2020. p.1-13. doi:10.1007/978-3-030-46781-4_1.
[54] Zhu J. Decision-oriented explainable artificial intelligence: A PDR-based review of methods, applications, and emerging frontiers. *Decision Making and Analysis*. 2026; 4(1): 87-99. doi:10.55976/dma.42026159087-99.
[55] Wolpert DH, Macready WG. No free lunch theorems for optimization. *IEEE Transactions on Evolutionary Computation*. 1997; 1(1): 67-82. doi:10.1109/4235.585893.
[56] Hossein Zadeh O, Hajjarian M, Reza Abdi M. Stakeholder bias and group decision dynamics: Mitigating cognitive biases with an integrated consensus-building process. *Decision Making and Analysis*. 2026; 4(1): 60-86. doi:10.55976/dma.42026146760-86.
[57] Blum C, Roli A. Metaheuristics in combinatorial optimization: Overview and conceptual comparison. *ACM Computing Surveys*. 2003; 35(3): 268-308. doi:10.1145/937503.937505.
[58] Venable J, Pries-Heje J, Baskerville R. FEDS: A framework for evaluation in design science research. *European Journal of Information Systems*. 2016; 25(1): 77-89. doi:10.1057/ejis.2014.36.
[59] Bazerman MH, Moore DA. *Judgment in Managerial Decision Making*. 8th ed. Hoboken (NJ): John Wiley & Sons; 2012.
[60] Kahneman D, Tversky A. Prospect theory: An analysis of decision under risk. In: Baker HK, Nofsinger JR. (eds.) *Handbook of the Fundamentals of Financial Decision Making: Part I*. Singapore: World Scientific; 2013. p.99-127. doi:10.1142/9789814417358_0006.
[61] Rajinikanth V, Razmjooy N. A comprehensive survey of meta-heuristic algorithms. In: Razmjooy N, Ghadimi N, Rajinikanth V. (eds.) *Metaheuristics and Optimization in Computer and Electrical Engineering. Vol. 2, Hybrid and Improved Algorithms*. Cham: Springer; 2023. p.1-39. doi:10.1007/978-3-031-42685-8_1.
[62] Ma Z, Wu G, Suganthan PN, Song A, Luo Q. Performance assessment and exhaustive listing of 500+ nature-inspired metaheuristic algorithms. *Swarm and Evolutionary Computation*. 2023; 77: 101248. doi:10.1016/j.swevo.2023.101248.
[63] Hussain K, Mohd Salleh MN, Cheng S, Shi Y. Metaheuristic research: A comprehensive survey. *Artificial Intelligence Review*. 2019; 52(4): 2191-2233. doi:10.1007/s10462-017-9605-z.
[64] Rodríguez Carrillo ML, Pérez-Domínguez L, Romero-López R, Luviano-Cruz D, León-Castro E. A systematic literature review on the use of multicriteria

decision-making methods for small and medium-sized enterprises innovation assessment. *Frontiers in Artificial Intelligence*. 2025; 8: 1605756. doi:10.3389/frai.2025.1605756.

[65] Milkman KL, Chugh D, Bazerman MH. How can decision making be improved? *Perspectives on Psychological Science*. 2009; 4(4): 379-383. doi:10.1111/j.1745-6924.2009.01142.x.

[66] Hodgkinson GP, Healey MP. Psychological foundations of dynamic capabilities: Reflexion and reflection in strategic management. *Strategic Management Journal.* 2011; 32(13): 1500-1516. doi:10.1002/smj.964.

[67] Shang Y. Subgraph robustness of complex networks under attacks. *IEEE Transactions on Systems, Man, and Cybernetics: Systems*. 2019; 49(4): 821-832. doi:10.1109/TSMC.2017.2733545.